

Elske de Zeeuw-van Dalfsen · Hazel Rymer ·
Glyn Williams-Jones · Erik Sturkell ·
Freysteinn Sigmundsson

Integration of micro-gravity and geodetic data to constrain shallow system mass changes at Krafla Volcano, N Iceland

Received: 27 August 2004 / Accepted: 7 July 2005 / Published online: 8 February 2006
© Springer-Verlag 2005

Abstract New and previously published micro-gravity data are combined with InSAR data, precise levelling and GPS measurements to produce a model for the processes operating at Krafla volcano, 20 years after its most recent eruption. The data have been divided into two periods: from 1990 to 1995 and from 1996 to 2003 and show that the rate of deflation at Krafla is decaying exponentially. The net micro-gravity change at the centre of the caldera is shown, using the measured free air gradient, to be $-85 \mu\text{Gal}$ for the first and $-100 \mu\text{Gal}$ for the second period. After consideration of the effects of water extraction by the geothermal power station within the caldera, the net gravity decreases are $-73 \pm 17 \mu\text{Gal}$ for the first and $-65 \pm 17 \mu\text{Gal}$ for the second period. These decreases are interpreted in terms of magma drainage. Following a Mogi point source model, we calculate the mass decrease to be $\sim 2 \times 10^{10}$ kg/year reflecting a drainage rate of $\sim 0.23 \text{ m}^3/\text{s}$, similar to the $\sim 0.13 \text{ m}^3/\text{s}$ drainage rate previously found at Askja volcano, N. Iceland. Based on the evidence for deeper magma reservoirs and the similarity between the two volcanic systems, we suggest a pressure-link between Askja and Krafla at deeper levels (at the lower crust or the crust-mantle boundary). After the

Krafla fires, co-rifting pressure decrease of a deep source at Krafla stimulated the subsequent inflow of magma, eventually affecting conditions along the plate boundary in N. Iceland, as far away as Askja. We anticipate that the pressure of the deeper reservoir at Krafla will reach a critical value and eventually magma will rise from there to the shallow magma chamber, possibly initiating a new rifting episode. We have demonstrated that by examining micro-gravity and geodetic data, our knowledge of active volcanic systems can be significantly improved.

Keywords Micro-gravity · Deformation · Krafla · Askja · Magma drainage · InSAR · Reservoir

Editorial responsibility: A. Harris

E. de Zeeuw-van Dalfsen (✉) · H. Rymer
Volcano Dynamics Group, Department of Earth Sciences, The
Open University,
Walton Hall, Milton Keynes, MK7 6AA, UK
e-mail: golfyankee@hotmail.com
Tel.: +44-1908659775
Fax: +44-1908655151

G. Williams-Jones
Department of Earth Sciences, Simon Fraser University,
Burnaby, British Columbia, Canada

E. Sturkell
The Icelandic Meteorological Office,
Reykjavik, Iceland

F. Sigmundsson
Nordic Volcanological Centre, Institute of Earth Sciences,
University of Iceland,
101 Reykjavik, Iceland

Introduction

The Northern Volcanic Zone north of the Vatnajökull ice cap in Iceland, consists of five NNE–SSW elongated volcanic systems: Theistareykir, Krafla, Fremri-Namur, Askja, and Kverkfjöll, (Fig. 1-inset). They are arranged en echelon along the plate boundary which is ~ 50 – 80 km wide. Each volcanic system consists of a fissure swarm transecting a central volcano.

The Krafla Volcanic System comprises a fissure swarm, which is 100 km long and ~ 10 km wide, more than 1,000 tectonic fractures, and a central volcano (Fig. 1). The Krafla central volcano forms a low, broad shield some 20 km in diameter with a caldera in the centre. The topographically indistinct caldera has an elliptical shape and stretches 10 km in the E–W direction and 8 km N–S. It formed during an explosive eruption in the last interglacial period about 0.1 Ma ago and has since been filled almost completely with lavas and ash (Brandadóttir et al. 1997).

Two geothermal areas, Krafla and Námafjall (Fig. 1) are located in the Krafla Volcanic System. Námafjall is located just south of the Krafla caldera on the eastern part of the Krafla fissure swarm. Its 3–4 km² surface expression is characterized by mud pools and fumaroles and three active

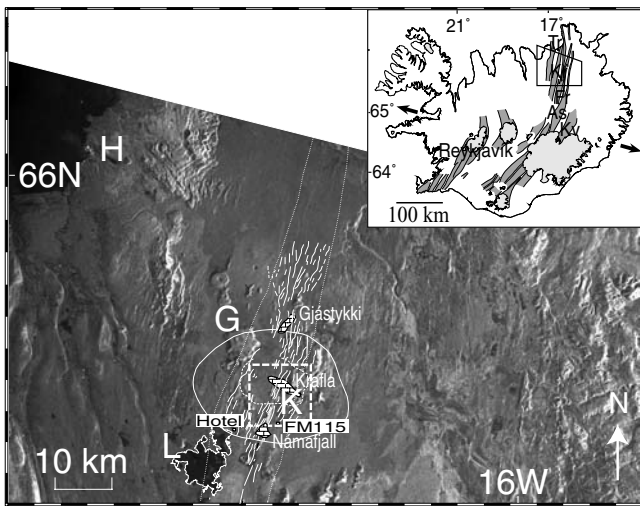


Fig. 1 Overview of the Krafla volcanic System, *inset* shows location of Krafla in Iceland. The locations of the main ice caps are depicted with *light grey* and the volcanic zones are depicted with *dark grey*. The *inset* also shows the five NNE–SSW elongated volcanic systems of the Northern Volcanic Zone, *Tr* Theystareykir, *Kr* Krafla, *Fr* Fremri-Namure, *As* Askja and *Kv* Kverkfjöll (Einarsson 1991). The *black box* marked on the *inset* shows the area covered by the enlargement given in the main figure. The larger figure shows the Krafla Rift Zone (*dotted*), the outline of the Krafla central volcano (*solid white line*), the caldera (*white dashed line*), the geothermal areas (*blocked*), the town of Husavik (*H*), lake Mývatn (*L*) and Krafla mountain (*K*) with a SAR amplitude image for reference in the background. Note the location of micro-gravity stations Hotel and FM115. *White dashed box* shows outline of Fig. 1

wells, with a maximum temperature of 320°C, which supply a 3 MW back-pressure turbine unit. The larger Krafla geothermal area, ~7 km², is located in the centre of the caldera and is elongated in the NW–SE direction. At present, 18 wells are used to operate a 60-MW power generator and geothermal fluid temperatures reach 350°C (Gudmundsson and Arnórsson 2002).

The activity at the Krafla volcanic system is characterised by rifting episodes separated by long periods of dormancy (e.g., Árnadóttir et al. 1998). Two historical rifting episodes, the so called Mývatn and Krafla fires, occurred from 1724 to 1729 and 1975 to 1984, respectively. During the Mývatn fires, the crater Víti was formed (Fig. 2), although most of the other activity manifested itself south of the Krafla caldera (Ewart et al. 1991). Activity resumed in 1975, when seismicity increased and deformation data suggested inflow of magma to the shallow Krafla reservoir, causing inflation followed by rapid deflation and an initial diking event (Tryggvason 1994). A rifting episode from 1975 to 1984 was then characterised by 21 such cycles of which 9 culminated in basaltic fissure eruptions (Björnsson 1985; Brandsdóttir et al. 1997). During each cycle, the reservoir pressure exceeded a critical value, reservoir walls failed, dykes were injected into the fissure swarm and rifting occurred. The largest and most voluminous eruption of this period occurred over two weeks in September 1984 during which an 8.5-km-long volcanic fissure erupted a pahoehoe lava field with a total area of 24 km² (Rossi 1997).

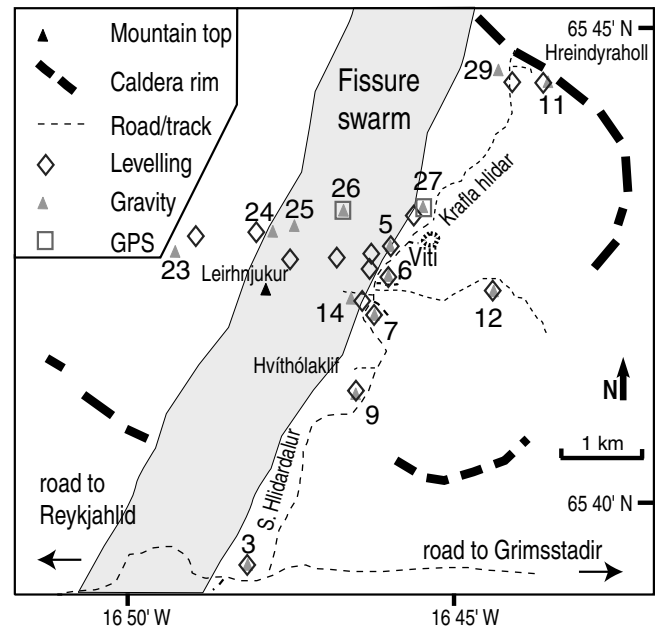


Fig. 2 Sketch of the location of the main micro-gravity, levelling and GPS stations at Krafla. Numbers refer to station names: 3 FM115, 5 OS5595, 6 5596, 7 OS5596, 9 5599A, 11 5672, 12 OS5684, 14 OS5688, 23 A001, 24 A002, 25 A003, 26 A004, 27 A005 and 29 A012

Krafla is one of the few calderas in the world—others include Askja in Iceland (Rymer and Tryggvason 1993), Masaya in Nicaragua (Williams-Jones et al. 2003), Poas in Costa Rica (Rymer et al. 2000) and Campi Flegrei in Italy (Gottsmann et al. 2003)—with a long-term micro-gravity data set. The area has also been studied extensively using a variety of geophysical techniques (Tryggvason 1986; Árnadóttir et al. 1998; Sigmundsson et al. 1997). Here we present Interferometric Synthetic Aperture Radar data (InSAR; 1993–1999) and micro-gravity data (1997–2003). Results of these techniques are combined to produce an integrated model for the processes operating at Krafla today, 20 years after the most recent eruption.

Methods

Geodetic methods

Previously published and new precise levelling, Global Positioning System (GPS) and InSAR data were combined to calculate the height change at each gravity station. InSAR allows the measurement of change in range from ground to satellite at a high spatial resolution by combining pairs of Synthetic Aperture Radar (SAR) images acquired at different acquisition times (Massonnet and Feigl 1995; Massonnet and Feigl 1998). Interferograms were produced with the use of the DIAPASON software (CNES 2000) following an approach similar to that used by Sigmundsson et al. (1997). Topographic fringes were removed with the help of a digital elevation model (DEM) from the Icelandic Geodetic Survey and orbital corrections were performed utilising

post-computed orbits from the European Space Agency (ESA). Residual orbital effects were removed by subtracting a linear range-change gradient. The remainder of the processing was done using sub-sections of the complete interferograms covering the Krafla area. These sections were filtered using an algorithm developed by Z. Lu (personal communication 2002) and unwrapped using deformation tools developed by Gudmundsson et al. (2002). After unwrapping, the interferograms provide an unambiguous measure of the change in range whereas the original interferograms show deformation as fringes, each corresponding to a vertical displacement of 28 mm. The precise levelling technique measures the vertical deformation, with respect to reference station FM115, with millimetre precision (Fig. 1). Differential GPS measurements are referred to station NE9301 and have an accuracy in the vertical component of $\sim 1\text{--}2$ cm.

Micro-gravity methods

All the micro-gravity measurements discussed in this paper were acquired with the use of LaCoste & Romberg instruments following standard techniques as described by Rymer (1996). Meter G-513 has been used for all surveys since 1990 and its calibration characteristics are well known (Carbone and Rymer 1999); meter G-403 has been used in addition since 1997. The micro-gravity network traditionally uses station Hotel (Fig. 1) as reference, because it is located outside the main zone of deformation (Rymer et al. 1998). Station FM115 has also been measured on a regular basis. Although its location near the central axis of the plate boundary is not ideal, it has been used here as an alternative reference station to better coordinate with the deformation network. The uncertainty expected for this type of micro-gravity survey considering the climate, time delay between readings, and jolting of the instruments during transport is $10\text{--}20 \mu\text{Gal}$ (Rymer 1989). Repeat measurements have been made during this study and the uncertainties for the newly acquired data are displayed in Table 2. Before we can interpret the micro-gravity data in terms of mass movements, they need to be corrected for height with the use of geodetic data. The free air gradient (FAG) is the change of gravity with elevation and is used to calculate the expected gravity change at each station due to the height changes alone. The FAG varies depending on the local sub-surface mass distribution. The local value of the FAG can be determined in the field following the methodology of Rymer (1996) and is used here to calculate net gravity changes.

Data and results

Deformation data

The Krafla system is subject to deformation because of the stresses associated with the divergent plate boundary, the effects of magma movements and geothermal

processes. The recent extensive geothermal exploitation and production at the Krafla power station also influences the system. Any deformation data collected will necessarily reflect the complex interaction between all these processes.

Previous results

No significant ground deformation changes were observed in data from the 1938 to 1965 period (Björnsson et al. 1979). Between 1965 and 1971, apparent contraction took place followed by extension and uplift between 1970 and 1975 (Moller and Ritter 1980; Rymer et al. 1998). The Krafla power plant was under construction at that time and geodetic surveys and exploration drillings had started in 1974. Levelling profiles crossing the caldera region were available from the very beginning of the 1975–1984 rifting episode. Ground deformation was monitored extensively during the episode (Ewart et al. 1991), using a wide range of techniques such as electronic distance measurements (EDM; Tryggvason 1994), precise levelling (Björnsson 1985) and tilt and lake level measurements (Tryggvason 1986; Tryggvason 1994). Deformation during the rifting episode was characterised by steady inflation interrupted by rapid subsidence (Tryggvason 1994). After the last eruption in September 1984, slow inflation was observed from 1985 to 1989. This was followed by subsidence, initially at a rate of ~ 5 cm/year, declining to ~ 2.5 cm/year in 1992–1995 (Tryggvason 1994; Sigmundsson et al. 1997; Árnadóttir et al. 1998; Rymer et al. 1998).

Radar interferometry (InSAR) has also been used successfully in the Krafla region to monitor deformation (Sigmundsson et al. 1997; Henriot et al. 2001; de Zeeuw-van Daltsen et al. 2004a). Analysing interferograms covering the 1992–1995 period, Sigmundsson et al. (1997) observed 2.4 cm/year of subsidence in the centre of the Krafla area and ~ 0.7 mm/year along axis subsidence of the spreading segment. Henriot et al. (2001) analysed interferograms from the 1992–1998 period and found steady subsidence at Krafla and the fissure swarm of 1.9 cm/year (2.1 cm/year in the ground to satellite direction). Based on interferometric data from 1993 to 1999, de Zeeuw-van Daltsen et al. (2004a) showed the existence of a wide inflating area in addition to the already suggested subsiding zones.

New data

Integration of the new GPS and InSAR data with previously published geodetic data is complicated by the fact that different groups acquired the data, using different reference stations and with several temporal gaps in the data set. To alleviate this problem, all data are first normalised to the same base station (FM115; Figs. 1 and 2) and yearly height changes are calculated for each gravity station (Table 1), interpolating and extrapolating where necessary.

Table 1 Total height change data for 1990 to 2003 based on the precise levelling surveys reported by Björnsson and Eysteinnsson (1998) and Ágústsson (2001). Numbers refer to location of station, for coordinates see Table 2 (also partly displayed on Fig. 2). An ‘a’ in the first column means the levelling station is close to but not identical to the gravity station with that number, but height change data from

the a-station are used to correct for height changes at the corresponding gravity station. Method of estimation is described in text. Note that the negative numbers here reflect deflation. These should not be confused with the decreasing rate of deflation shown in Fig. 3. The standard deviation on the data is 1.5 cm which corresponds to $\sim 5 \mu\text{Gal}$ (based on the average FAG $\sim 310 \pm 12 \mu\text{Gal/m}$)

No	Levelling station	Estimated height change 1990–1995 (m)	Levelling 1995–2000 Ágústsson (m)	Estimated height change 2000–2003 (m)	Total height change 1990–2003 (m)
3	FM115	0.000	0.000	0.000	0.000
5	OS5595	-0.074	-0.019	-0.005	-0.097
6	5596	-0.086	-0.041	0.001	-0.126
7	OS5597	-0.061	-0.022	0.001	-0.083
8	5599	-0.013	-0.003	0.000	-0.015
9	5599A	-0.013	-0.003	0.000	-0.015
10	OS5600	-0.002	0.004	0.000	0.002
11	5672	0.013	0.037	0.000	0.049
12	OS5684	-0.052	-0.000	0.001	-0.052
13	OS5685	-0.054	0.007	0.001	-0.046
15	OS5697	-0.000	0.004	0.000	0.004
16	OS5698	0.002	0.003	0.000	0.005
17	OS5699	0.001	0.003	0.000	0.004
1a	KONGSP	0.017	0.014	0.000	0.032
14a	KB08	-0.075	-0.032	0.001	-0.106
14a	KB11	-0.088	-0.030	0.001	-0.117
23a	KV08	-0.079	-0.007	0.001	-0.085
24a	KV12	-0.097	-0.025	0.001	-0.120
25a	KV02	-0.111	-0.028	0.002	-0.137
26a	LV956104	-0.085	-0.028	0.001	-0.112
27a	FM5670	-0.054	-0.011	0.001	-0.064
29a	LV956107	0.108	0.035	-0.001	0.141

First order levelling surveys conducted in the Krafla area in 1989, 1995 and 2000 (Björnsson and Eysteinnsson 1998; Magnússon 2003) form the basis of our deformation model. The data exceed the requirements for height correction of the gravity data as they have a standard deviation of less than 1.5 cm and the levelling stations are equivalent or close to the micro-gravity stations (Rymer 1996). We consider two distinct periods, 1990–1995 and 1996–2003, in order to take into account change in productivity of the geothermal power plant from 30 to 60 MW between 1995 and 1996 (Hauksson and Benjamínsson 2003).

Twelve SAR images from the European Remote Sensing (ERS) satellites 1 and 2 (track 9, frame 2277), acquired during the 1993–2000 period, allowed the formation of twelve interferograms, with reasonable coherence. The four with the best coherence were selected for modelling and the average subsidence rate over the time period (spanning from 2 to 6 years) was inferred. Overall, the subsidence rate calculated from these data decays from ~ 1.5 cm/year in late 1996 to ~ 1.1 cm/year in late 1997.

Previous work indicates that the deformation rate at Krafla has been decaying rapidly since 1989 (Tryggvason 1994). In order to extrapolate the deformation data at Krafla from 2000 to 2003, it is important to know the trend of this decay. The vertical change over a time period obtained from different measurements by several authors is expressed as a rate (cm/year) in Fig. 3. The points may be

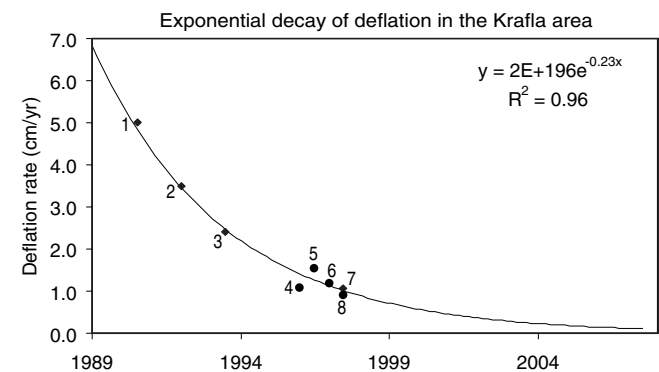


Fig. 3 Exponential decay of deflation in cm in the area of maximum deflation at Krafla. Numbers refer to publications: 1 (Tryggvason 1994), 2 (Björnsson and Eysteinnsson 1998), 3 (Sigmundsson et al. 1997), 4–6 and 8 (this paper) and 7 (Ágústsson 2001)

fitted by two straight lines or by an exponential curve. We prefer an exponential fit because the subsidence is expected to show exponential behaviour like the subsidence at other Icelandic volcanoes (Sturkell and Sigmundsson 2000). A good fit through the data with a root mean square of 0.96, is found using estimates for average maximum subsidence from published data (Tryggvason 1994; Sigmundsson et al. 1997; Björnsson and Eysteinnsson 1998; Ágústsson 2001; Henriot et al. 2001) together with the newly acquired

Table 2 Coordinates and micro-gravity data (in mGal) for stations in the monitoring network. Numbers refer to location on map (partly displayed in Fig. 2). Station names starting with A and NE were installed by the Nordic Volcanological Institute, stations Hotel and

Helluhraun by the Open University and the remainder by the National Energy Authority of Iceland. *SD* standard deviation (μGal), in brackets in data column

No	Station name	Latitude	Longitude	2002		2003	
				Meter G-403	Meter G-513	Meter G-403	Meter G-513
1	Hotel	N65°38'42.0"	W016°54'55.1"	15.436(9)	15.501(7)	15.412(25)	15.518(35)
2	Helluhraun	N65°38'31.1"	W016°54'28.2"	13.311(22)	13.367(1)	13.279(18)	13.395(7)
3	FM115	N65°38'40.6"	W016°48'08.8"	0.000	0.000	0.000	0.000
4	2313	N65°38'40.8"	W016°48'08.9"	13.311(−)	−0.014(5)	−0.021(−)	−0.032(7)
5	OS5595	N65°42'51.5"	W016°45'59.7"	−30.667(8)	−30.761(18)	−30.688(21)	−30.770(16)
6	5596	N65°42'27.2"	W016°46'01.5"	−14.740(1)	−14.769(10)	−14.757(16)	−14.766(0)
7	OS5597	N65°41'56.7"	W016°46'14.2"	−13.222(5)	−13.274(20)	−13.239(16)	−13.260(35)
8	5599	N65°40'54.8"	W016°46'30.9"	−0.179(22)	−0.172(5)	−0.241(−)	−0.184(−)
9	5599A	N65°40'53.2"	W016°46'35.8"	−0.186(21)	−0.211(12)	−0.228(33)	−0.220(18)
10	OS5600	N65°40'20.4"	W016°47'02.4"	−0.479(17)	−0.492(14)	−0.507(−)	−0.455(20)
11	5672	N65°44'28.1"	W016°43'36.9"	−52.051(11)	−52.215(10)	−52.137(−)	
12	OS5684	N65°42'16.1"	W016°44'26.3"	−45.946(−)	−46.078(−)	−45.932(−)	−46.087(−)
13	OS5685	N65°42'08.2"	W016°43'38.0"	−48.230(−)	−48.382(−)	−48.266(−)	−48.382(−)
14	OS5688	N65°42'08.6"	W016°46'35.9"	−13.669(31)	−13.688(2)	−13.662(10)	−13.706(5)
15	OS5697	N65°39'51.5"	W016°47'33.5"	−0.378(16)	−0.358(14)	−0.385(12)	−0.337(34)
16	OS5698	N65°39'30.7"	W016°47'38.4"			−0.127(39)	−0.103(38)
17	OS5699	N65°39'00.8"	W016°47'31.0"	0.152(2)	0.144(3)	0.150(6)	0.168(23)
18	OS5843	N65°41'12.9"	W016°46'41.8"	−15.402(10)	−15.46(21)	−15.435(20)	−15.478(−)
19	NE220	N65°38'13.8"	W016°48'33.6"	−1.377(24)	−1.380(−)	−1.398(21)	−1.338(22)
20	NE9301	N65°41'24.8"	W016°46'31.0"	−13.027(1)	−13.074(18)	−13.061(−)	−13.036(−)
21	NE80051	N65°41'34.5"	W016°45'25.6"	−35.776(−)	−35.864(−)	−35.790(−)	
22	NE79077	N65°42'34.3"	W016°46'34.5"	−34.424(29)	−34.496(4)	−34.445(6)	−34.498(7)
23	A001	N65°42'42.8"	W016°49'14.7"	−31.580(20)	−31.664(43)	−31.669(−)	−31.644(−)
24	A002	N65°43'01.5"	W016°47'46.5"	−39.750(18)	−39.861(27)	−39.794(−)	−39.876(−)
25	A003	N65°43'06.5"	W016°47'26.9"	−39.053(27)	−39.161(17)	−39.121(−)	−39.181(−)
26	A004	N65°43'18.3"	W016°46'42.9"	−28.013(13)	−28.055(7)	−28.056(13)	−28.028(16)
27	A005	N65°43'21.1"	W016°45'29.5"	−31.030(25)	−31.113(29)	−31.088(57)	−31.097(−)
28	A008	N65°44'12.7"	W016°44'54.3"	−34.510(−)	−34.659(−)	−34.628(−)	
29	A012	N65°44'37.7"	W016°44'18.5"	−58.327(8)	−58.487(4)	−58.373(−)	15.518(−)
Average SD				14	12	19	12

results from InSAR (Fig. 3). Since the micro-gravity stations do not coincide with the assumed location of maximum subsidence caused by the shallow magma chamber, the extrapolated height change data (for the period post 2000) also need to be interpolated (spatially). This is done by noting the distribution of measured elevation changes in the 1997–1998 period (middle of the 1995–2000 levelling period) compared to the predicted maximum deformation from the decay curve (Fig. 3). The same decay curve is also used to interpolate data for those stations lacking levelling data from 1990 to 1995. Finally, the curve is used to extract the 1990 to 1995 deformation from the 1989 to 1995 levelling data. Estimated deformation in 1989 has been subtracted from the 1989–1995 measured value. The total deformation (Table 1) at each levelling station relative to base station FM115 is then calculated by adding the results from the levelling (or interpolated values) from 1990 to 2000 and the extrapolated values from 2000 to 2003. Because each micro-gravity station is the same or close to a levelling station, these values are used to interpret the

micro-gravity data. The standard deviation is estimated, based on repeated measurements, to be 1.5 cm for the vertical component. In summary, results from geodetic surveys in the Krafla region after 1998, show that the Krafla volcanic system is still deflating. The deflation at Krafla follows an exponential decay trend and, assuming there is no change in activity, is expected to reach the detection limit by 2007.

The total volume change at the surface, ΔV_e , can be calculated from the deformation data most simply by assuming a Mogi model (Mogi 1958) where the deformation is caused by a pressure change of a point source within an elastic half-space, (Johnson 1987):

$$\Delta V_e = 2\pi \Delta h \frac{(r^2 + d^2)^{3/2}}{d} \quad (1)$$

The maximum subsidence, Δh , at the centre of the deformation relative to station FM115 is -0.085 m from 1990 to 1995 and -0.024 m from 1996 to 2003. The average

depth to the source, d , is 2,800 m as inferred from previous geodetic modelling (Sigmundsson et al. 1997; Árnadóttir et al. 1998; Rymer et al. 1998). The horizontal distance from the centre of deformation to this source, r , is 1,300 m in the 1990–1995 period and 2,000 m in the 1996–2003 period. FM115 is located within the deformation zone and any estimates for ΔV_e are therefore minimum values. InSAR data covering most of this period (de Zeeuw-van Dalfsen et al. 2004a) indicate that the subsidence does not extend beyond this region and therefore the volume calculated for ΔV_e is considered to be realistic. ΔV_e is calculated to be -0.006 km^3 for the 1990 to 1995 period and -0.002 km^3 for the 1996 to 2003 period.

Micro-gravity

The first micro-gravity measurements in the Krafla region were made in 1965 (Björnsson et al. 1979) and extensive work was done during the beginning of the 1975–1984 rifting episode (Johnsen et al. 1980). Since then, micro-gravity measurements have been made yearly at Krafla from 1990 to 1997, with the exception of 1993 (Rymer et al. 1998), and again in 2002 and 2003.

The 29 main micro-gravity stations (partly displayed in Fig. 2 and Table 2) at Krafla can be grouped according to location: Hreindýrahóll (5672, A008 and A012), Leirhnjúkur (A001, A002, A003 and A004), Hlídar Krafla (OS5595, 5596, 5597, OS5688, NE79077 and A005), Hvíthólaklif (5599, 5599a, OS5843, NE9301 and NE80051) and South Hlíðardalur (NE220, OS5697, OS5698, OS5699 and OS5600). There are four control or base stations (Hotel, FM115, Helluhraun and 2313) and two stations that fall outside these groups (OS5684 and OS5685).

Previous results

Rymer et al. (1998) investigated post-eruptive gravity changes from 1990 to 1996 inclusively. After corrections for elevation change, significant net gravity decreases on the order of $-50 \text{ } \mu\text{Gal}$, were observed over the modelled Mogi-type deflation source. Net gravity increases up to $60 \text{ } \mu\text{Gal}$ were observed 1–3 km from the centre of deformation. In addition to this, here the effect of water extraction has been taken into account for the 1990–1996 period.

Gottsmann and Rymer (2002) analysed $\Delta g/\Delta h$ gradients for all available data from 1977 to 1996. Their theory suggests that the relationship between the measured gradient, the free air gradient (FAG) and the Bouguer corrected free air gradient (BCFAG) predicts which process is responsible for caldera unrest.

New results

The micro-gravity network at Krafla (Fig. 2, Table 2) was re-measured during the summers of 1997, 2002 and

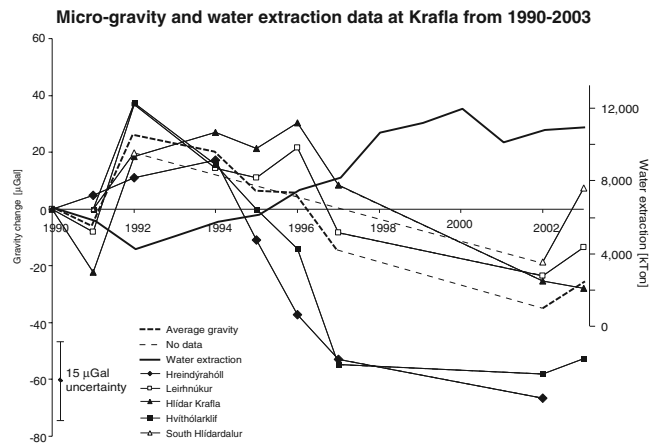


Fig. 4 Micro-gravity and water extraction data for Krafla between 1990 and 2003. Micro-gravity data are referred to base station FM115 and relative to 1990. The names of the station groups refer to locations plotted in 2. The *thick dashed line* shows the average gravity. The average standard deviation on all data through all years is $15 \text{ } \mu\text{Gal}$. Total yearly water extraction data are taken from the National Energy Authority of Iceland (Hauksson and Benjamínsson 2003)

2003 using station FM115 as a reference and the results are presented here. The average standard deviation of all measurements is 14 and $12 \text{ } \mu\text{Gal}$ in 2002 and 19 and $18 \text{ } \mu\text{Gal}$ in 2003 (Table 2), for meters G-403 and G-513, respectively.

During the 2002 survey, the FAG was measured at several key stations as suggested by Gottsmann and Rymer (2002). The results show a FAG close to the theoretical value for the reference station (FM115) and the South Hlíðardalur stations. Across the rift, the FAG differs considerably, with values of $-386 \pm 12 \text{ } \mu\text{Gal/m}$ in the Leirhnjúkur area and $-280 \pm 12 \text{ } \mu\text{Gal/m}$ in the Hreindýrahóll area (Table 3). This difference is caused by topographic variations and the local Bouguer anomalies. The measured FAG values were then contoured to allow the FAGs at the unmeasured stations to be estimated.

A comparison of the 2002 and 2003 data with earlier surveys (Fig. 4) reveals that there has been a micro-gravity increase at the Leirhnjúkur, Hlídar Krafla and South Hlíðardalur stations from 1990 to 1996 averaging to about $\sim 25 \text{ } \mu\text{Gal}$. This is followed by a relative micro-gravity decrease of $\sim 45 \text{ } \mu\text{Gal}$ from 1996 to 2002 and a small increase of $\sim 10 \text{ } \mu\text{Gal}$ from 2002 to 2003. At the Hreindýrahóll and Hvíthólaklif stations, micro-gravity data show an increase of $\sim 20 \text{ } \mu\text{Gal}$ from 1990 to 1994, followed by a steep decrease of $80 \text{ } \mu\text{Gal}$ from 1994 to 1997. No change occurred from 1997 to 2002 and from 2002 to 2003 these stations show a micro-gravity increase of $\sim 10 \text{ } \mu\text{Gal}$. The average of all gravity stations is also depicted in Fig. 4 (broken line). For gravity changes to be considered significant, they need to exceed $15 \text{ } \mu\text{Gal}$. There is some (non-linear) trend in the gravity change signal in Fig. 4 but before any interpretation can be made, the effects of height changes need to be considered.

Table 3 Calculation of the net micro-gravity change for the 1990–1995 and 1996–2003 periods. Numbers refer to location on map (Fig. 2). FAG values without superscripted are values measured at that station ($\pm 12 \mu\text{Gal/m}$). Station names in brackets are the nearest levelling station if different from gravity station.

No	Name	FAG [$\mu\text{Gal/m}$]	1990–1995			1996–2003			Net Δg [μGal]	Measured Δg [μGal]	Expected Δg [μGal]	Net Δg [μGal]
			Height change [cm]	Expected Δg [μGal]	Measured Δg [μGal]	Net Δg [μGal]	Height change [cm]	Expected Δg [μGal]				
1	Hotel (KONGSP)	-0.310	4.482	-14	35	49	1.720	-5	19		25	
3	FMI15	-0.300	0.000	0	0	0	0.000	0	0		0	
5	OS5595	-0.314	-6.082	19	-1	-20	-2.334	7	-73		-81	
6	5596	-0.322 ^a	-13.125	42	35	-7	-5.036	16	-3		-20	
7	OS5597	-0.322 ^a	-7.043	23	72	49	-2.702	9	-62		-71	
9	5599A	-0.304	-0.960	3	30	27	-0.369	1	-55		-56	
11	5672	-0.290 ^a	11.844	-34	-5	29	4.545	-13	-33		-20	
12	OS5684	-0.347	0.480	-2	15	17	0.184	-1	-104		-104	
14	OS5688 (KB08&11)	-0.330 ^a	-10.244	34	52	19	-3.931	13	-48		-61	
23	A001 (KV08)	-0.365 ^a	7.683	-28	41	69	2.948	-11	-42		-31	
24	A002 (KV12)	-0.375 ^a	1.921	-7	15	22	0.737	-3	-61		-58	
25	A003 (KV02)	-0.386	0.960	-4	12	16	0.369	-1	-77		-75	
26	A004 (LV956104)	-0.348 ^a	-8.963	31	-55	-86	-3.439	12	5		-7	
27	A005 (FM5670)	-0.315 ^a	-3.521	11	-23	-34	-1.351	4	-14		-19	
29	A012 (LV956107)	-0.280	11.204	-31	-13	19	4.299	-12	-53		-41	

^aValues have been estimated from contours

Bold numbers represent net gravity decreases

Calculation of net micro-gravity

The net micro-gravity changes were calculated using the measured values of the FAG where possible (Table 3), or with estimates derived from the contoured FAG values. The vertical motion at each station is multiplied by the FAG to calculate the expected micro-gravity change. Subtraction of the expected changes due to vertical motion from the measured micro-gravity changes yields the net micro-gravity change due to changes in sub-surface mass. The net micro-gravity changes for the two periods under consideration are most easily visualised on contour maps (Fig. 5). Station 5596 was excluded from the contouring during the 1996–2003 period because the net gravity decrease found at this location is small ($-20 \mu\text{Gal}$) compared to that found at nearby gravity stations ($\sim -75 \mu\text{Gal}$). A reason for this

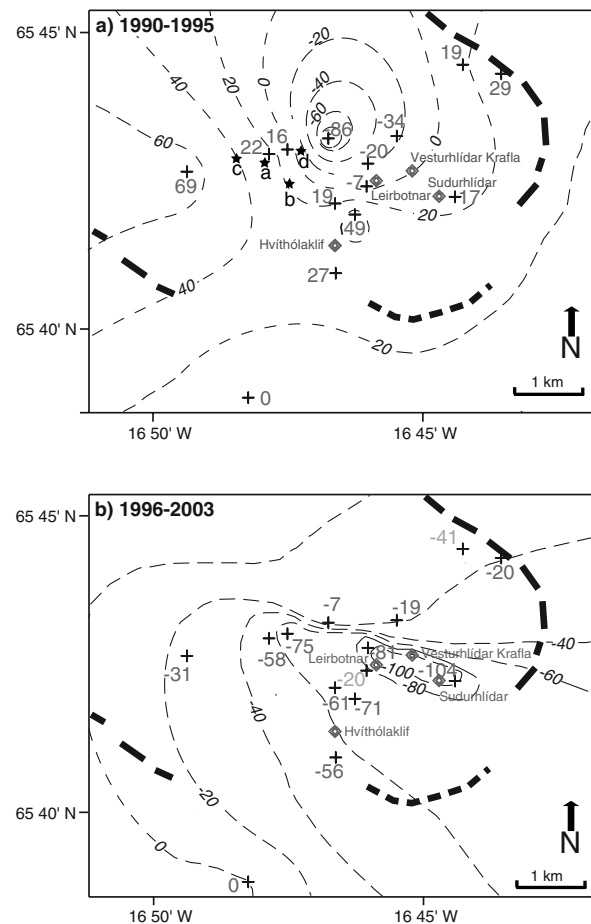


Fig. 5 **a** Net micro-gravity contours (in μGal) at Krafla from 1990 to 1995 following data from Table 3. Gravity stations are represented by a cross and numbers refer to values as in Table 3. Diamonds represent drill holes for water extraction. Positive contours are dashed while negative contours are solid lines. The thick dashed line shows the caldera rim. The area of net gravity decrease is located in the centre of the caldera. Suggested locations of possible shallow magma chamber (see Table 4) are depicted with black stars *a*, *b*, *c* and *d*. **b** Net micro-gravity contours (in μGal) at Krafla from 1996 to 2003 following data from Table 3 and same symbols as **a**. Note that the anomalous data points FM5596 and A012 have not been taken into account during the contouring. Area of net gravity decrease is concentrated around the drill hole sites

Water extraction from drill holes in the Krafla area
1990 to 2003

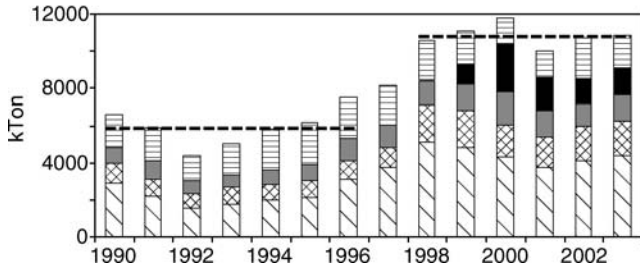


Fig. 6 Water extraction from drill holes in the Krafla area from 1990 to 2003 (Hauksson and Benjamínsson 2003). Note that extraction has doubled since 1998 compared to the 1990–1996 period. Names refer to locations of drill sites as used in Fig. 5 □ Leirbotnar; ■ Hvíthólaklif; ▤ Bjarnarflag; ▨ Sudurhlíðar; ▩ Vesturhlíðar

could be that this gravity station is closest to the drill-hole site where, in 2002, 1,400 kt of water was injected into the system.

There is an important contrast between the 1990–1995 and 1996–2003 data. During the 1990 to 1995 period, a net gravity decrease of $-85 \mu\text{Gal}$ was concentrated around the Leirhnúkur stations. This coincides with the location of the latest activity during the Krafla fires and suggests it may have been caused by magmatic processes. During the 1996 to 2003 period, almost all stations show a net micro-gravity decrease. An E–W elongated feature with a maximum net gravity decrease of $-100 \mu\text{Gal}$ can be identified. This area correlates well with the location of the drill-hole sites. Processes responsible for the observations could include (1) influences of the geothermal power plant: water mass extraction and the increased cooling rate of the shallow magma body (causing contraction) caused by the increased water circulation and (2) drainage of magma from a shallow magma body.

Influence of the geothermal power plant

Water extraction (dotted line in Fig. 4) has been increasing steadily since 1992 (Hauksson and Benjamínsson 2003). The average yearly water extraction of $\sim 6,000$ kt for the 1990–1996 period, increased to $\sim 11,000$ kt for the 1998–2003 period (Fig. 6). There is a clear inverse correlation between the average gravity and the water extraction (Fig. 4).

The fact that there are net micro-gravity changes suggests that sub-surface mass changes are occurring. Sub-surface mass decrease could be caused by movement of the steam-water interface, drainage of magma from a reservoir or extraction of geothermal water at the Krafla power plant. Movement of the steam-water interface can not be excluded but its influence will be too small to explain the observed mass changes (Gottsmann and Rymer 2002). We suggest the two alternative explanations are more likely causes. In order to better understand the non-magmatic influence on the gravity signal, we consider in more detail the extraction of water at the geothermal power plant (Fig. 6).

From 1990 to 2002, a total of 7.94×10^3 kt (7.94×10^{10} kg) water was extracted at the various drill holes (Hauksson and Benjamínsson 2003). The drill holes are co-located with the micro-gravity network (Fig. 5) and are concentrated at five sites located (1) south of the caldera in Bjarnarflag, (2) at Hvíthólaklif, (3) in the centre of the caldera (near the power plant), (4) at Leirbotnar, and (5) south of the Krafla mountain at Sudurhlíðar Krafla. The extraction of water was more or less constant from 1981 to 1996, but subsequently almost doubled due to the increased demand caused by the installation of the second turbine in 1996. To complicate the mass balance picture even further, injection of water *into* the system was initiated in 1999. This did not contribute considerably until 2002 when injection amounted to 1,400 kt/year. This may account for the small increase in raw gravity observed from 2002 to 2003.

The Krafla geothermal system consists of two separate geothermal zones at different depths (Stefánsson 1981). The shallower of the two is avoided during exploitation of the field because of its lower temperature and association with calcite deposition. The top of the $\sim 1,000$ -m-thick deeper zone is located around 1,100–1,300 m.

The gravitational effect of the water extraction in the Krafla area can be simulated by a cylinder with changing density in the same way as used by Hunt (1970) for the Wairakei geothermal field in New Zealand. The density change, σ , can be calculated as follows:

$$\sigma = \frac{\Delta m}{(\pi r^2 h)} \quad (2)$$

The mass change in kg, Δm , in the centre of the caldera (excluding Bjarnarflag), is -2.28×10^{10} kg from 1990 to 1995 and -6.57×10^{10} kg from 1996 to 2003. The radius of the cylinder or the effected area, r , varies from 100 to 10,000 m. The height of the cylinder or the thickness of the aquifer, h , is 100 m.

The gravitational effect, Δg , on the surface above the centre of this cylinder can then be calculated as follows (Parasnis 1979):

$$\Delta g = 2\pi G\sigma [h_2 - z + \sqrt{r^2 + z^2} - \sqrt{r^2 + h_2^2}] \quad (3)$$

where G , is the gravitational constant, of 6.67×10^{-11} Nkg²/m². The depth of the cylinder, z , from the surface to the top of the aquifer, varies from 100 to 1,300 m. h_2 is the depth to the bottom of the cylinder, in metres. Equation 3 is empirical and variations in g will be caused by variations in z , h_2 and r .

The results of the calculations are shown in Fig. 7. The average estimate of the gravitational effect of the water extraction from 90 to 1995 is approximately $-12 \mu\text{Gal}$, assuming the extraction affects an area with a radius of 4 km. This is the approximate radius of the caldera and the aquifer is known to exist as a broad layer within this region (Stefánsson 1981). This effect is smaller than the average standard deviation on the data set and may therefore not be detectable. For the period of 1996–2003, the estimated

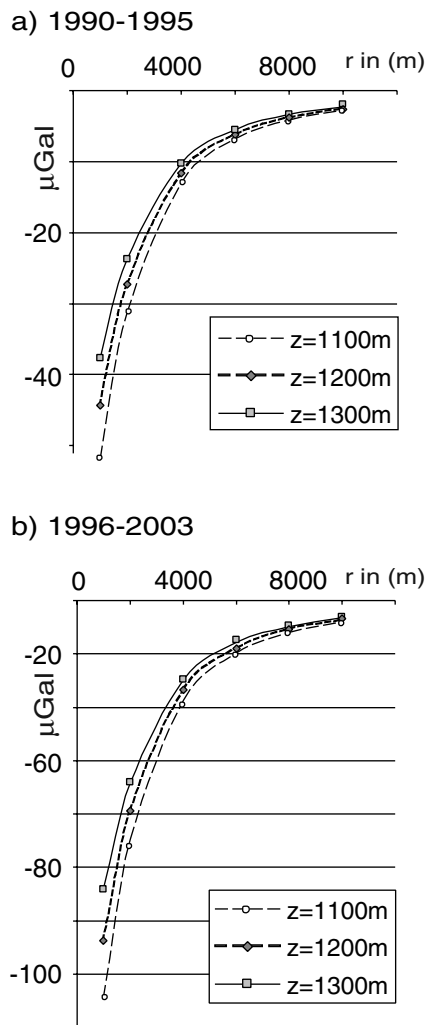


Fig. 7 Micro-gravity effect of water drainage in μGal for the two periods. z is the depth to the top of the cylinder, i.e., the depth to the top of the aquifer, varying from 1,100 mm to 1,300 m. The thickness of the aquifer is 1,000 m and r is the radius of the cylinder

gravitational effect is approximately $-35 \mu\text{Gal}$, assuming the same area is affected. This effect is larger than the average standard deviation and should therefore be measurable and visible in the data set. Since we ignore the flow of water into the area from the surroundings to accommodate the water extraction, the estimated gravitational effects are maximum values.

Interpretation

Geodetic data

Over the years, several deformation models have been developed using data acquired with a range of geodetic techniques (Table 4, Fig. 2). All of these models include a Mogi point source sometimes referred to as the Krafla magma reservoir. Its location varies only slightly between models, although depth is less well constrained. Analysis of

local earthquakes (Einarsson 1978) defined two regions of shear wave attenuation, which were inferred as a shallow magma reservoir, although this study did not define the magma reservoir in any detail. Brandsdóttir and Menke (1992) showed the presence of a low velocity zone that is interpreted as the shallow magma reservoir, less than 1 km thick with its top at a depth of approximately 3 km. However, it is not possible to explain all the observed deformation with this one point source, especially at an increased distance from the source. Therefore, several types of additional sources have been suggested to complement the model (Table 4). All micro-gravity stations lie within the zone mostly influenced by the point source and by the extraction of the geothermal resources, and therefore for the context of this work, only the Mogi source and geothermal field will be considered.

Subsidence observed in interferograms spanning the 1993–1999 period (de Zeeuw-van Dalssen et al. 2004a), is consistent with a Mogi source deflating at a rate of $\sim 0.3 \times 10^6 \text{ m}^3/\text{year}$. This process is envisaged as deflation of the shallow Krafla magma reservoir. Over the same period, a deeper inflating Mogi source, further north and at 21 km depth, inflated at a rate of $\sim 26 \times 10^6 \text{ m}^3/\text{year}$. The inflating source is at or near the crust-mantle boundary as identified by seismic studies and is interpreted as accumulating magma (de Zeeuw-van Dalssen et al. 2004a).

Gravity data

Rymer et al. (1998) interpreted the observed (1990–1996) net gravity decrease at Krafla as magma drainage of at least $4 \times 10^{10} \text{ kg}$ and the net gravity increases as the result of a migrating steam-water interface and/or closure of micro-fractures during post-eruptive cooling and contraction. Gottsmann and Rymer (2002) emphasised, however, that the net gravity increases were not only associated with a density increase, but also were accompanied by a mass increase of $\sim 10^{10} \text{ kg}$. They suggested that magma moved laterally out of the reservoir into dykes.

The inverse correlation between micro-gravity and water extraction data (Fig. 4) suggests water extraction has an important influence on the mass balance of the system and therefore on the gravity data. Furthermore, the fact that gravity is decreasing in areas of general deflation indicates that sub-surface mass decreases may be occurring. The influence of the water extraction by the geothermal power plant is also obvious in 1996–2003 (Fig. 5). There may be a volcanic signal hidden within these data, but before this can be observed, data should be corrected for the water extraction.

The calculated net gravity decrease from 1990 to 1995 is $-85 \pm 12 \mu\text{Gal}$ (to correct for the influence of water extraction) which leads to a still significant net-gravity decrease of $-73 \pm 17 \mu\text{Gal}$ (RMS of gravity readings is $\pm 16 \mu\text{Gal}$, RMS of deformation data is $\pm 6 \mu\text{Gal}$, $\sqrt{16^2 + 6^2} = 17$). Since the effects of water drainage have been taken into account, this mass decrease is most likely caused by magma drainage over the 6-year period. From

Table 4 Model data for a Mogi point source as reported by various authors throughout the years. *EDM* Electronic Distance Measurements; *InSAR* Interferometric Synthetic Aperture Radar

Reference	Parameters of Mogi source			Additional source	Input data
	Latitude(°)	Longitude(°)	Depth (km)		
Björnsson (1985)	–	–	–	Molten layer 5–7 km feeding shallow reservoir	Magneto-telluric
Trygvasson (1986) see star a, Fig. 5	65.715	16.797	2.6	Three more stacked reservoirs, at 5–10 km, >20 km and deeper	EDM, lake level, tilt
Rymer et al. (1996) same as star a, Fig. 5	65.715	16.797	~2.5		EDM, lake level, tilt
Sigmundsson et al. (1997) see star b, Fig. 5	65.71	16.79	3	Line source	InSAR
Árnadóttir et al. (1998) see star c, Fig. 5	65.715	16.806	~3	Dike	EDM, tilt, height differences
De Zeeuw-van Dalftsen et al. (2004a) see star d, Fig. 5	65.72	16.78	~2.4	Mogi 2 at 65.83 °N, 16.73 °W, line source	InSAR

1996 to 2003 the calculated net gravity decrease is $-100 + 35 \mu\text{Gal}$ (to correct for the influence of water extraction) which culminates in a significant net gravity decrease of $-65 \pm 17 \mu\text{Gal}$ over the 8-year period.

The mass change (ΔM) within a spherical (point source) body, whose depth is much greater than its radius, causes a gravitational effect on the surface (Δg) that is related to its mass change (ΔM) by (Dzurisin et al. 1980; Johnson 1987; Rymer and Tryggvason 1993):

$$\Delta M = \frac{\Delta g(r^2 + d^2)^{3/2}}{Gd} \quad (4)$$

where G is the Universal gravitational constant of $6.67 \times 10^{-11} \text{ Nm}^2/\text{kg}^2$. The depth to the point source, d , is 2,800 m as estimated by geodetic modelling (Tryggvason 1986; Sigmundsson et al. 1997; Árnadóttir et al. 1998; Rymer et al. 1998). The horizontal distance to this source, r , is 1,300 m from 1990–1995 and 2,000 m from 1996–2003 (i.e. the horizontal distance from the point source to the area with maximum net gravity change).

In the following text, we refer to edifice volume changes (ΔV_e) and relate them to sub-surface magma volume changes (ΔV_m) and magma chamber volume changes (ΔV_{ch}). Following Eq. 4, a mass decrease of $1.1 \times 10^{11} \text{ kg}$ occurred from 1990–1995, followed by a decrease of $1.4 \times 10^{11} \text{ kg}$ from 1996 to 2003. This is equivalent to magma drainage of $\sim 2 \times 10^{10} \text{ kg/year}$ visualised as a continuous ongoing process. After correction for the water extraction, the two periods show very similar drainage rates and, because drainage is visualized as a continuous process, we prefer to interpret the data in terms of volume changes for the whole period at once. Assuming a density of $2,700 \text{ kg/m}^3$ for the sub-surface magma body, the total mass decrease represents a minimum change in magma outflow volume (ΔV_m) of -0.09 km^3 from 1990 to 2003.

Earlier (see section Deformation data, Previous results), we calculated the total volume change at the surface (ΔV_e) from 1990 to 2003 to be -0.008 km^3 . This volume change comprises a combination of volume change caused by wa-

ter extraction, cooling/contraction of the magma reservoir and/or magma drainage from the magma reservoir. Because ΔV_e is dependent on the maximum subsidence at the centre of the caldera (h in Eq. 1), the curve following the decay of deformation is also representative for ΔV_e . This suggests that ΔV_e was not significantly influenced by water extraction, as data would not follow a smooth line if influenced by a significant change in water extraction between 1995 and 1996. Therefore, we argue that there is no need to correct ΔV_e for water extraction. Following Johnson et al. (2000), the corresponding sub-surface volume change of the Mogi source (ΔV_{ch}) is two thirds of the surface deflation volume or -0.005 km^3 . InSAR modelling (de Zeeuw-van Dalftsen et al. 2004a) at Krafla suggests a total volume change of the deflating Mogi source of the same order of magnitude (-0.002 km^3 for the 1993–1999 period).

Comparing this value with the calculated total change in Mogi source volume (ΔV_m) we find that the magma drainage volume is actually 17 times larger than the Mogi source volume. It has been suggested that volumetric decompression of stored magma may be caused by the variation in reservoir pressure accompanying magma drainage (Johnson 1992; Johnson et al. 2000). The net volume change of the stored magma, ΔV_c , changes because of this decompression. A combination of reduction of the reservoir size, ΔV_{ch} , and decompression of the stored magma, ΔV_c would accommodate the magma drainage. Although not our preferred explanation, part of the volume discrepancy could also be explained by boiling in the geothermal system and density decrease in excess of that suggested only from extracted water.

Discussion and conclusions

The results from this work show significant mass decreases at the Krafla caldera which we interpret in terms of magma drainage. The Krafla caldera is located on the Northern Volcanic Zone in Iceland and as such is part of a larger volcanic system. It is therefore important to extend our interpretation and discussion beyond the Krafla area. In the

past three years, more and more data covering the Northern Volcanic Zone have been analysed. To advance our knowledge of volcanic processes, it is important to use all available information.

The Askja volcanic centre in the Dyngjufjöll central volcano (Sigvaldason 2002) hosts three calderas, the largest one being the circular Askja caldera. Askja volcano is located 80 km south of the Krafla volcanic system but is also located on the divergent spreading plate boundary in N. Iceland. The most recent eruption began there in October 1961 and continued into early December of the same year. de Zeeuw-van Dalssen et al. (2004b) found a net micro-gravity decrease of 115 μGal at Askja caldera, corresponding to a sub-surface mass decrease of 1.6×10^{11} kg between 1988 and 2003. They suggested the mass decrease of $0.125 \text{ m}^3 \text{ s}^{-1}$ was due to magma drainage from a shallow reservoir. They suggest that extensional tectonic forces generate space in the ductile lower crust to accommodate drainage (of degassed magma) from the shallow magma chamber to deeper levels. The work presented here suggests a mass decrease of 2.5×10^{11} kg, implying a drainage rate of $0.23 \text{ m}^3 \text{ s}^{-1}$ at Krafla from 1990 to 2003, which is of the same order of magnitude as that at Askja. We suggest that pressure reduction along the plate boundary due to the plate spreading process can accommodate this ongoing magma drainage from the shallow magma chamber. Links between the two volcanoes have been suggested by several authors (Tryggvason 1986; Rymer and Tryggvason 1993; Sturkell et al. 2004—accepted).

Deflation at both the Askja and Krafla volcanoes is decaying through time. However, while Askja has been deflating with an average rate of 5 cm/year between 1988 and 2003, Krafla deflated at only 1 cm/year between 1990 and 2003. Also, the $\Delta V_m/\Delta V_{ch}$ ratio at Askja for the 1988–2003 period is 3, roughly five times smaller than the ratio estimated for Krafla (17) for the 1990–2003 period. A possible explanation for this difference might be the existence of the extensive geothermal system at Krafla, cooling the volcanic system more rapidly.

Recently, re-evaluation of new and previously published geodetic data at both volcanoes suggests a best fit for models with two stacked magma reservoirs. For Askja, Sturkell et al. (2004—accepted) suggested two magma reservoirs at 3 and 16 km depth; while at Krafla, de Zeeuw-van Dalssen et al. (2004a) suggested the existence of deep magma accumulation at 21 km depth in addition to a magma reservoir at 2.8 km depth. It is possible that a pressure-link between these volcanoes exists along the ductile lower crust in Iceland. We suggest that after the Krafla fires, co-rifting pressure decrease of the deeper source stimulated the subsequent inflow of magma. This inflow might influence conditions along the plate boundary as far away as Askja, 70 km to the south. The pressure of the deeper reservoir at Krafla will reach a critical value and eventually magma will rise to the shallow magma chamber, possibly initiating a new rifting episode. The last significant eruptive period at Krafla before 1974 was in 1724–1729 and this may indicate the timescale for replenishment of the upper magma chamber.

It is possible that not only Icelandic but also other volcanoes located on a constructive plate boundary are interconnected at depth. Several authors have suggested connections between volcanoes in other parts of the world in all types of tectonic settings, but the suggested connections are mostly shallow in nature. At Mauna Loa and Kilauea in Hawaii, the possible connection between the two volcanoes remains controversial. Recently, Miklius and Cervelli (2003) suggested a crustal-level interaction between the two magma systems based on a short timescale correlation found in continuous deformation data.

This paper has demonstrated the power of using a range of techniques simultaneously to study volcanoes. We have shown it can improve the understanding of the ongoing processes at the studied volcano as well as offering constraints on the dynamics of, and linkages through, the volcanic system at a broader scale. We anticipate that using a range of techniques concurrently will considerably increase our knowledge of volcanic systems in the future.

Acknowledgements This work was supported by The Geological Society, London and an Open University studentship. H.R.'s work on this project (1990–2003) was supported by the Royal Society. We would like to thank all the people that have participated in collection of the data at Krafla, especially Ton de Zeeuw, Andrew J. Ball and Halldór Ólafsson who helped during the most recent surveys. The geodetic work on this project was supported by a grant from the Icelandic Research Council RANNÍS and F.S.'s work on this project has been supported by the Retina project (EVG1-CT-00046). An earlier version of the manuscript was greatly improved by discussion with Dave Rothery and reviews by J.T. Freymueller and an anonymous reviewer.

References

- Ágústsson SM (2001) Landhæðarbreytingar á Kröflusvæðinu: hæðarmælingar 2000: samanburður við mælingar 1995. (in Icelandic). Háskóli Íslands, Reykjavík, 30 pp
- Árnadóttir T, Sigmundsson F, Delaney PT (1998) Sources of crustal deformation associated with the Krafla, Iceland, eruption of September 1984. *Geophys Res Lett* 25(7):1043–1046
- Björnsson A (1985) Dynamics of crustal rifting in NE Iceland. *J Geophys Res* 90:10151–10162
- Björnsson A, Eysteinnsson H (1998) Breytingar á landhæð við Kröflu 1974–1995. Samantekt á landhæðarmælingum. (in Icelandic). Nat. Energy Auth., Reykjavík OS-98002
- Björnsson A, Johnsen G, Sigurdsson S, Thorbergsson G (1979) Rifting of the plate boundary in north Iceland 1975–1978. *J Geophys Res* 84(B6):3029–3038
- Brandsdóttir B, Menke W (1992) Thin low-velocity zone within the Krafla caldera, NE Iceland attributed to a small magma chamber. *Geophys Res Lett* 19:2381–2384
- Brandsdóttir B, Menke W, Einarsson P, White RS, Stapels RK (1997) Färoe-Iceland ridge experiment 2: crustal structure of the Krafla central volcano. *J Geophys Res* 102(B4):7867–7886
- Carbone D, Rymer H (1999) Calibration shifts in a LaCoste-and-Romberg gravimeter: comparison with a Scintrex CG-3M. *Geophys Prospect* 47(1):73–83
- CNES (2000) Installation guide for DIAPASON. Centre National d'études spatiales, Toulouse
- de Zeeuw-van Dalssen E, Pedersen R, Sigmundsson F, Pagli C (2004a) Satellite Radar Interferometry 1993–1999 suggests deep accumulation of magma near the crust-mantle boundary at the Krafla volcanic system, Iceland. *Geophys Res Lett* 31(13):L13611, doi:10.1029/2004GL020059

- de Zeeuw-van Dalfsen E, Rymer H, Sigmundsson F, Sturkell E (2004b) Net gravity decrease at Askja volcano, Iceland: constraints on processes responsible for continuous caldera deflation, 1988–2003. *J Volcanol Geotherm Res* 139:227–239
- Dzurisin D, Anderson LA, Eaton GP, Koyanagi RY, Lipman PW, Lockwood JP, Okamura RT, Puniwai GS, Sako MK, Yamashita KM (1980) Geophysical observations of Kilauea Volcano, Hawaii, 2: constraints on the magma supply during November 1975–September 1977. *J Volcanol Geotherm Res* 7(3–4):241–269
- Einarsson P (1978) S-wave shadows in the Krafla caldera in NE-Iceland, evidence for a magma chamber in the crust. *Bull Volcanol* 41:1–9
- Einarsson P (1991) Earthquakes and present day tectonism in Iceland. *Tectonophysics* 189:261–279
- Ewart JA, Voight B, Björnsson A (1991) Elastic deformation models of Krafla Volcano, Iceland, for the decade 1975 through 1985. *Bull Volcanol* 53:436–459
- Gottsmann J, Berrino G, Rymer H, Williams-Jones G (2003) Hazard assessment during caldera unrest at the Campi Flegrei, Italy: a contribution from gravity-height gradients. *Earth Planet Sci Lett* 211:295–309
- Gottsmann J, Rymer H (2002) Deflation during caldera unrest: constraints on subsurface processes and hazard prediction from gravity-height data. *Bull Volcanol* 64(5):338–348
- Gudmundsson BT, Arnórsson S (2002) Geochemical monitoring of the Krafla and Námafjall geothermal areas, N. Iceland. *Geothermics* 31:195–243
- Gudmundsson S, Carstensen JM, Sigmundsson F (2002) Unwrapping ground displacement signals in satellite radar interferograms with aid of GPS data and MRF regularization. *IEEE Transact Geosci Remote Sensing* 40(8):1743–1754
- Hauksson T, Benjaminsson J (2003) Krafla og Bjarnarflag Afköst borhola og efnainnihald vatns og gufu í borholum og vinnslurás ári 2002 (in Icelandic). Rep. Landsvirkjun, Kröflustö, pp 1–70
- Henriot O, Villemain T, Jouanne F (2001) Long period interferograms reveal 1992–1998 steady rate of deformation at Krafla volcano (North Iceland). *Geophys Res Lett* 28(6):1067–1070.
- Hunt TM (1970) Net mass loss from the Wairakei geothermal field, New Zealand. *Geothermics* 2(1):487–491
- Johnsen GV, Björnsson A, Sigurdsson S (1980) Gravity and elevation changes caused by magma movement beneath Krafla caldera, northeast Iceland. *J Geophysics* 47:132–140
- Johnson D (1987) Elastic and inelastic magma storage at Kilauea volcano. In: *Volcanism in Hawaii*, vol 2, United States Government printing Office, Washington, pp. 1297–1306
- Johnson DJ (1992) Dynamics of magma storage in the summit reservoir of Kilauea volcano, Hawaii. *J Geophys Res* 97(B2):1807–1820
- Johnson DJ, Sigmundsson F, Delaney PT (2000) Comment on 'Volume of magma accumulation or withdrawal estimated from surface uplift or subsidence, with application to the 1960 collapse of Kilauea volcano' by P.T. Delaney and D.F. McTigue. *Bull Volcanol* 61:491–493
- Magnússon IP (2003) Þyngdarmælingar við Kröflu árid 2000 (in Icelandic). Internal report Landsvirkjun, Orkustofnun, OS-2003/06
- Massonnet D, Feigl K (1995) Discrimination of geophysical phenomena in satellite radar interferograms. *Geophys Res Lett* 22(12):1537–1540
- Massonnet D, Feigl K (1998) Radar interferometry and its application to changes in earth's surface. *Rev Geophys* 36(4):441–500
- Miklius A, Cervelli P (2003) Interaction between Kilauea and Mauna Loa. *Nature* 421:229
- Mogi K (1958) Relations between the eruptions of various volcanoes and the deformations of the ground surfaces around them. *Bull Earthquake Res Inst* 36:99–134
- Moller D, Ritter B (1980) Geodetic measurements and horizontal crustal movements in the rift zone of NE Iceland. *J Geophys* 47(1–3):110–119
- Rossi MJ (1997) Morphology of the 1984 open-channel lava flow at Krafla volcano, northern Iceland. *Geomorphology* 20:95–112
- Rymer H (1989) A contribution to precision microgravity data-analysis using Lacoste and Romberg gravity meters. *Geophys J* 97(2):311–322
- Rymer H (1996) Microgravity monitoring. In: *Monitoring and mitigation of volcano hazards*, Springer, Berlin Heidelberg New York, pp. 169–198
- Rymer H, Cassidy J, Locke CA, Barboza MV, Barquero J, Brenes J, Van der Laat R (2000) Geophysical studies of the recent 15-year eruptive cycle at Poas Volcano, Costa Rica. *J Volcanol Geotherm Res* 97(1–4):425–442
- Rymer H, Cassidy J, Locke CA, Sigmundsson F (1998) Post-eruptive gravity changes from 1990 to 1996 at Krafla volcano, Iceland. *J Volcanol Geotherm Res* 87(1–4):141–149
- Rymer H, Tryggvason E (1993) Gravity and elevation changes at Askja, Iceland. *Bull Volcanol* 55(5):362–371
- Sigmundsson F, Vadon H, Massonnet D (1997) Readjustment of the Krafla spreading segment to crustal rifting measured by satellite radar interferometry. *Geophys Res Lett* 24(15):1843–1846
- Sigvaldason GE (2002) Volcanic and tectonic processes coinciding with glaciation and crustal rebound: an early Holocene rhyolitic eruption in the Dyngjufjoll volcanic centre and the formation of the Askja caldera, north Iceland. *Bull Volcanol* 64(3–4):192–205
- Stefánsson V (1981) The Krafla geothermal field, northeast Iceland. In: *Geothermal systems: principles and case histories*. Wiley, New York, pp. 273–294
- Sturkell E, Sigmundsson F (2000) Continuous deflation of the Askja caldera, Iceland, during the 1983–1998 noneruptive period. *J Geophys Res* 105(B11):25671–25684
- Sturkell E, Sigmundsson F, Slunga R (2004) 1983–2003 decaying rate of deflation at Askja caldera: pressure decrease in an extensive magma plumbing system at a spreading plate boundary. *Bull Volcanol*
- Tryggvason E (1986) Multiple magma reservoirs in a rift-zone volcano: ground deformation and magma transport during the September 1984 eruption of Krafla, Iceland. *J Volcanol Geotherm Res* 28(1–2):1–44
- Tryggvason E (1994) Surface deformation at the Krafla volcano, North Iceland, 1982–1992. *Bull Volcanol* 56:98–107
- Williams-Jones G, Rymer H, Rothery DA (2003) Gravity changes and passive SO₂ degassing at the Masaya caldera complex, Nicaragua. *J Volcanol Geotherm Res* 123:137–160